

# **THE DESIGN, ASSEMBLY, AND TESTING OF AN ACTIVE ROTARY FLUX COMPRESSOR**

Prepared by

M.L. Spann, W.L. Bird, W.F. Weldon, and H.H. Woodson

Presented at

The 3rd IEEE International Pulsed Power Conference  
Albuquerque, New Mexico

June 1-3, 1981



Publication PN-72

Center for Electromechanics  
The University of Texas at Austin  
Balcones Research Center  
Bldg. 133, EME 1.100  
Austin, TX 78758  
512/471-4496

# THE DESIGN, ASSEMBLY, AND TESTING OF AN ACTIVE ROTARY FLUX COMPRESSOR

M. L. Spann, W. L. Bird, W. F. Weldon, and H. H. Woodson

Center for Electromechanics  
The University of Texas at Austin  
Taylor Hall 167  
Austin, Texas 78712

## Summary

A 20-cm diameter rotor active rotary flux compressor has been fabricated at the Center for Electromechanics, the University of Texas at Austin, (CEM-UT) to verify the predicted advantages of fully laminated ferromagnetic rotor and stator construction. An unsaturated flux compression ratio ( $L_{max}/L_{min}$ ) of 46:1 has been achieved. Measured inductance values verify space harmonic magnetic field distribution code predictions. Under short circuit testing pulse widths less than 600  $\mu s$  and current gains in excess of 15:1 have been obtained at a rotor speed of 63 percent of the first rotor critical speed.

## Introduction

Since February 1978 the Center for Electromechanics, the University of Texas at Austin, (CEM-UT) has pursued the compensated pulsed alternator (compulsator) program to develop less-expensive pulsed power supplies for driving loads with pulse widths less than 1 ms.<sup>1,2,3</sup> Typical loads of interest include nonlinear resistors (500  $\mu s$ -1 ms) and capacitors (<100  $\mu s$ ). A 200 kJ engineering prototype compulsator was designed and fabricated in 1979 to demonstrate the feasibility of driving xenon flashlamps for pumping solid state lasers. Initial discharge tests in December 1979 verified the pole face eddy current losses reduced performance to approximately 68 percent of the original design goal.<sup>3</sup> CEM-UT suggested that the performance level could be increased by laminating the stator structure, to obtain ferromagnetic boundaries on both sides of the air gap. To minimize cost and reduce lead time it was proposed to demonstrate the benefits of a fully laminated design on a smaller-scale device.

Therefore, the stator of an existing 20-cm brushless rotary flux compressor (BRFC)<sup>2</sup> was rewound to match the winding of a new laminated rotor armature. A photograph of the machine, rewound as an active rotary flux compressor (ARFC), is shown in Figure 1. The machine was constructed for static impedance measurements. However, existing ball bearings were used to position the rotor in the stator assembly. Later in 1981 it became advantageous to actually spin the rotor and perform short circuit discharge tests.

## Design Philosophy

The ARFC was designed as a static measurement device to verify the performance predictions of the space harmonic distribution model. In order that comparisons to the prototype compulsator could be made there were many similarities of design. The ARFC has a four-pole rotating armature winding wound in a modified wave winding configuration. An identical stationary winding is bonded to the stator bore and is connected in series with the armature winding through the armature brushes. The windings are similar to those of the prototype compulsator in terms of number of poles, winding configuration, and span width of the poles.

To reduce eddy current losses and to improve the inductance variation the stator was laminated over the active length of the winding. In the end-turn region

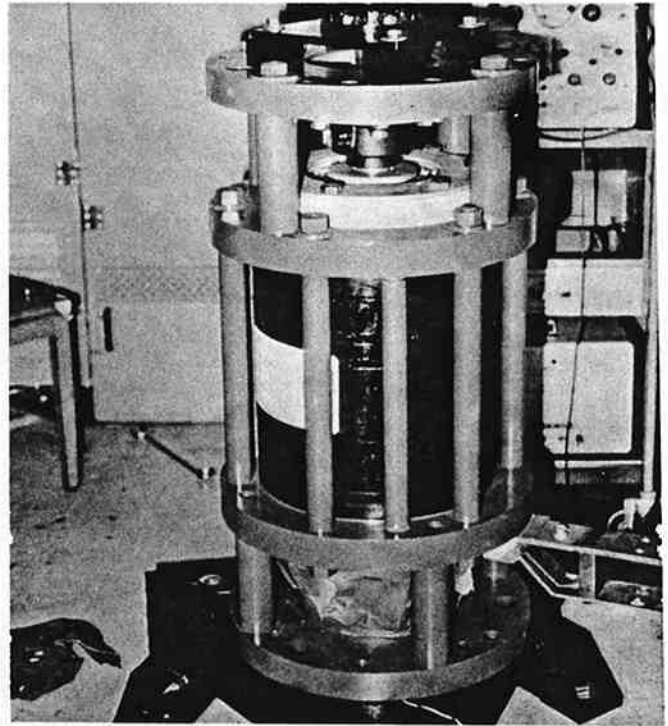


Fig. 1. Active Rotary Flux Compressor

the laminations represent shorted turns for eddy currents. Therefore efforts were made on both the rotor and stator to shield the laminations and all solid steel materials from the end turns. As shown in Figure 2 the end turns are wound over a nonmagnetic insulating material. This helps limit the amount of flux that reaches the laminations and other conductive materials. In addition .317-cm-thick copper sheets were used to shield the laminations and steel plates. The copper represents a low resistance path for eddy currents to flow and terminate the end-turn flux.

The rotor was also designed with a taper over the end-turn region. The diameter of the rotor decreases at a rate of 0.025 cm/cm of length. This had the effect of increasing the air gap in the end-turn region, thereby increasing the dielectric strength of the machine.

## Rotor

In order to reduce eddy current resistive losses the rotor is composed of approximately 900 nonoriented silicon sheet steel (M-19) laminations. The laminations are .036-cm thick and 18.6 cm in diameter. The laminations are insulated using a military refinish concentrate that phosphatizes the surface. The laminations were then shrunk fit onto a 6.35-cm, 4340-steel shaft.

In designing the laminated rotor it was necessary to keep the first natural frequency above the design speed. Calculations showed that the stiffness of the solid shaft alone was insufficient. Therefore it was necessary to compress the laminations in order to

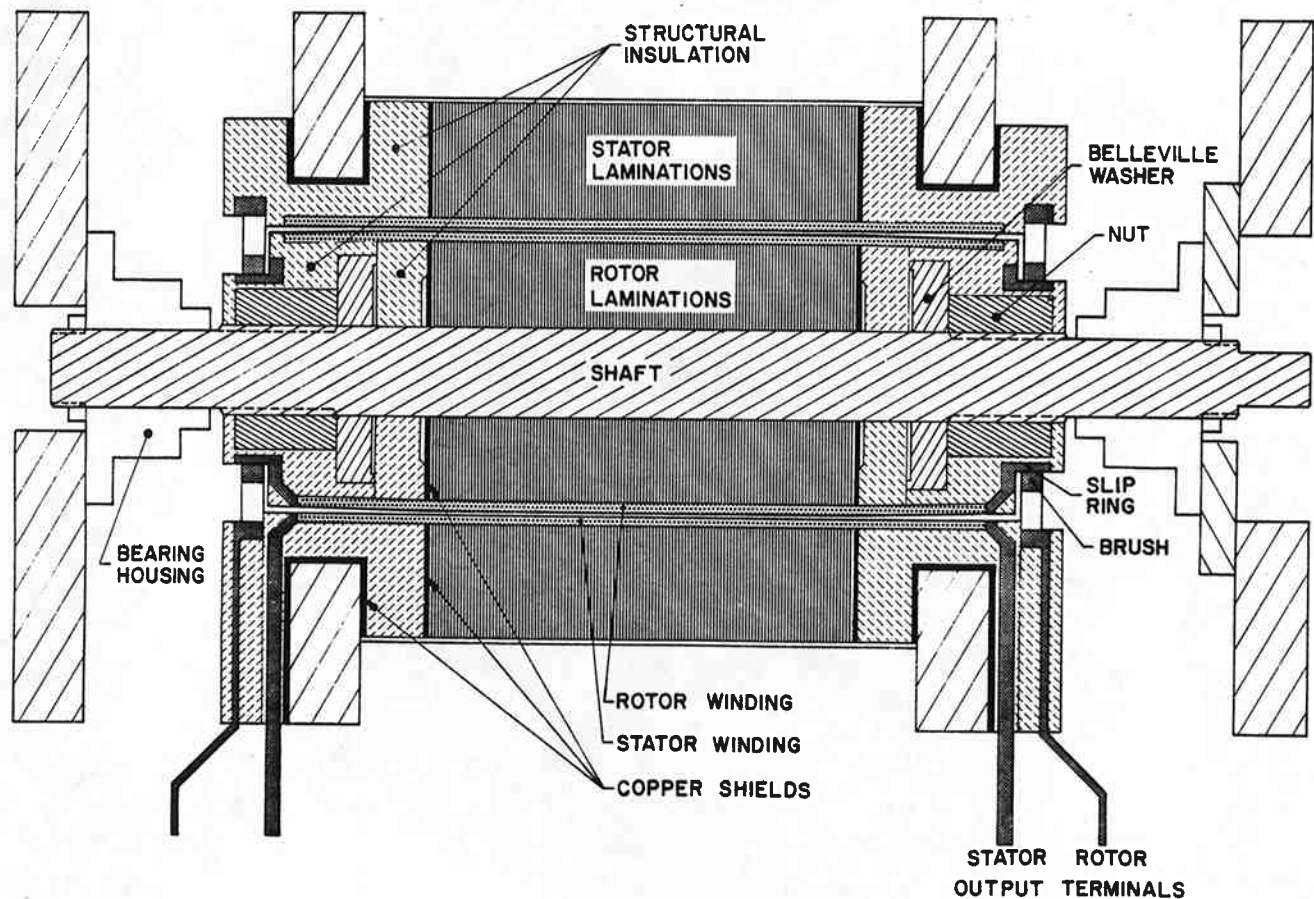


Fig. 2. Design Layout of ARFC (KD-20)

increase the rotor stiffness.

As shown in Figure 3 the rotor was treated as a simple supported beam with varying material properties and cross-sections. Solving the above system yields the stiffness

$$K_{\text{rotor}} = \left[ 5 \frac{b^3}{E_1 I_1} + 5 \frac{b^2 a}{48 E_1 I_1} + \frac{b a^2}{4 E_1 I_1} + \frac{a^3}{6 E_2 I_2} \right]^{-1}$$

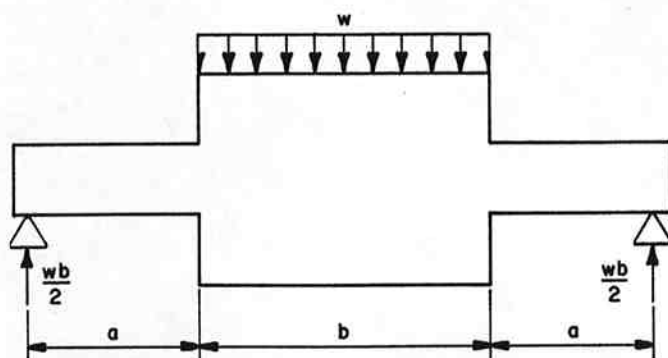


Fig. 3. Model of laminated rotor (KD-19)

Using this equation the rotor stiffness was calculated to be  $6.99 \times 10^7$  N/m. For the 375 kg rotor the natural frequency was calculated to be 946 rad/s. After assembly the actual natural frequency of the rotor was measured using a Hewlett Packard 5420A digital signal analyzer and found to be 1005 rad/s. After several days the rotor had relaxed to a natural frequency of 949 rad/s.

The laminations are clamped using two 4140 steel

Belleville washers. The washers are 16.5 cm in diameter and 2.62-cm thick and designed to provide a  $8.88 \times 10^5$  N load at a stroke of .104 cm. The nuts, made of 4340 steel, are 7.3-cm thick and 11.43 cm in diameter. The nuts were tightened, compressing the Belleville washers, using a large impact wrench.

#### Stator

The stator was constructed of laminations similar to those used in the rotor construction. The laminations are 0.036-cm thick and have a 38.1-cm outer diameter. After they were dipped in the phosphate conversion solution, the laminations were sprayed with epoxy, stacked, and compressed to form a solid unit. The laminations were then bored to a 21.8-cm inner diameter. The lamination stack was originally built and used for a BRFC under contract with the Naval Surface Weapons Center.<sup>2</sup>

#### Windings

The rotor and stator windings are four poles with 12 turns per pole. Due to the nature of the modified wave winding one pole contains only eleven turns making a total of 47 turns. Each turn consists of five parallel type 8 Litz wires.

The rotor was ground to its final dimension of 18.623 cm and acid etched to prepare the surface for bonding. The rotor was then wrapped with a stage B epoxy fiberglass tape. The tape was half-lap wrapped over the rotor forming the ground plain insulation and the winding spacers. After curing and machining to diameter, slots were milled out of the insulation for the windings. The rotor was wound with Litz wire con-

sisting of 14 strands of No. 22 AWG magnet wire. Before curing, the rotor was half-lap wrapped with stage B epoxy fiberglass tape, pretensioned glass fiber banding, and mica mat tape.

The stator windings were laid in the bore of the laminated stator. Ground plane insulation of stage B epoxy fiberglass tape was laid linearly in the bore. Spacers were cut from fiberglass tape wound over a mandrel and cured. The spacers were laid in the bore and wedged in place while the winding was accomplished. A half-lap wrap of mica mat tape formed the air-gap insulation. An expanding mandrel was inserted to compress the epoxy tape sufficiently to form a good bond.

#### Static Impedance Measurements

After the ARFC was assembled static measurements of the armature circuit inductance and resistance were made to verify inductance calculations and to determine the effectiveness of the design modifications to limit stray eddy current losses. Complex impedance values were determined using a Hewlett Packard 5420 A digital signal analyzer. Measurements were made at several frequencies (up to 3 kHz) at the maximum inductance position. The complex impedance was also measured as a function of mechanical rotor angle at a constant frequency of 1 kHz. Since the reactance of the device is significantly greater than the resistance at the frequencies of interest, small errors in phase angle result in large errors in resistance measurements. Therefore it was necessary to correct the measured impedance for phase shift errors introduced by the current transformer and voltage divider.

The measured impedance values at 1 kHz are listed in Table I. Predicted values of inductance and dc resistance are provided for comparison. Note that measured values are listed for periods before and after the rotating short-circuit armature tests. In both cases the measured inductance values agree with the predicted values published in July 1980.<sup>4</sup> The predicted values were calculated using the space harmonic distribution code described in a companion paper.<sup>5</sup>

TABLE I  
Static Impedance Values

f = 1 kHz					
Parameter	Units	Date	Measured Value	Predicted Value	
$L_{\max}$ ( $\theta_m = \pi/2$ )	mH	9/24/80	1.09	1.19	
$L_{\min}$ ( $\theta_m = 0$ )	$\mu$ H	9/24/80	23.20	26.40	
$L_{\max}/L_{\min}$		9/24/80	46.90	45.10	
R dc	m $\Omega$	5/9/81	42.40	42.60	
$L_{\max}$ ( $\theta_m = -\pi/2$ )	mH	5/14/81	1.08		
$L_{\min}$ ( $\theta_m = 0$ )	$\mu$ H	5/14/81	24.00		
$R_{\max}$ ( $\theta_m = -\pi/2$ )	m $\Omega$	5/14/81	116-140 (depends on current level)		
$R_{\min}$ ( $\theta_m = 0$ )	m $\Omega$	5/14/81	42.70		

The inductances were calculated by multiplying the inductance per unit length obtained from the two-dimensional code by the actual machine dimensions. The length used for the maximum inductance is the length of the laminated section (active length). The length used for the minimum inductance is the average length of a conductor per pass, which includes the active length plus the end-turn length.

$$L_{\max} = 3.91 \text{ mH/m} \times 0.305 \text{ m} = 1.19 \text{ mH} (\theta_m = -\pi/2)$$

$$L_{\min} = 45.6 \text{ } \mu\text{H/m} \times 0.579 \text{ m} = 26.4 \text{ } \mu\text{H} (\theta_m = 0)$$

We have found this to be an acceptable method since the inductance per unit length at  $\theta_m = 0$  is relatively insensitive to the boundary conditions. Both regions then contribute almost equally to the total inductance. The inductance contributed by the end turns at  $\theta_m = -\pi/2$  is negligible, however, compared to the inductance over the active length. In the maximum inductance position the end turns generate primarily axial magnetic fields that are not enhanced by the laminated stack.

The armature inductance versus mechanical rotor angle  $\theta_m$  is plotted in Figure 4. Note that there are two relative minima and two relative maxima for the four-pole design. The relative minimum at  $\theta_m = -\pi$

is about 50 percent larger than the absolute minimum inductance because of the missing conductors in the modified wave winding.

(20 A p-p, f = 1.0 kHz)

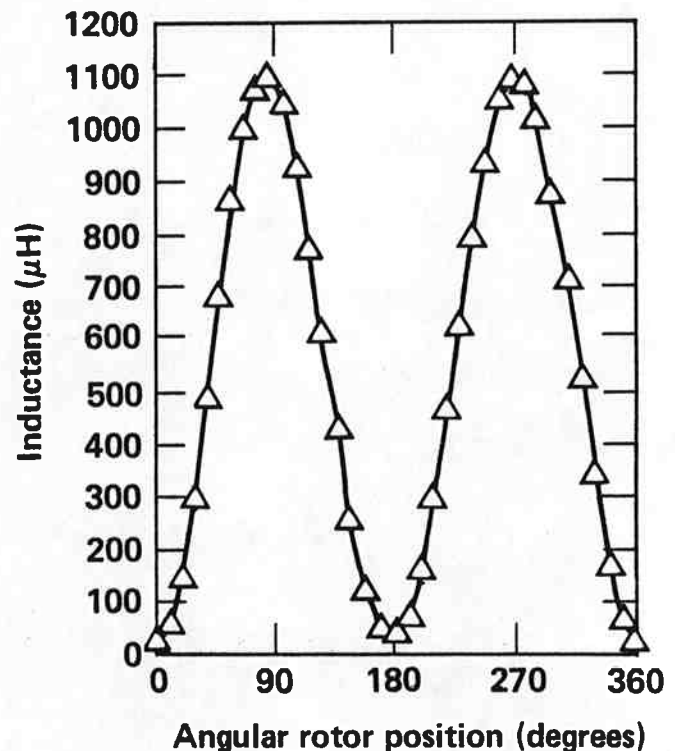


Fig. 4. Armature Inductance versus Rotor Position

#### Stray Eddy Current Losses

Although measured values of inductance varied less than ten percent over a frequency range of 500 Hz to 3 kHz, the effective resistance increased significantly at higher frequencies. This is due primarily to eddy current losses in the end-turn regions of the machine. These losses are attributable to eddy currents in the ferromagnetic shaft, shaft nut, Belleville washer, and stator support structure. At very high frequencies eddy currents over the active length of the rotor and stator also contribute to this loss as does proximity effect and circulating currents in the windings themselves. It is likely that the ac to dc resistance ratios of ten or higher could be expected at the maximum inductance position at 10 kHz. It will be necessary to reduce these losses to maintain energy delivery gain as pulsedwidths are reduced below 500  $\mu$ s.

## Short Circuit Discharge Tests

The ARFC described in this paper is approximately one-half scale compared to the engineering prototype compulsator. We have found from circuit analysis that a half-scale machine under short circuit conditions generates the same levels of current density and mechanical stress as a full-scale machine under load.

After the prototype compulsator armature winding was damaged during open circuit voltage tests, we proposed to test the ARFC under short circuit loading using the capacitor bank ignitron, and diode array from the prototype compulsator experiment. A simplified schematic diagram is shown in Figure 5.

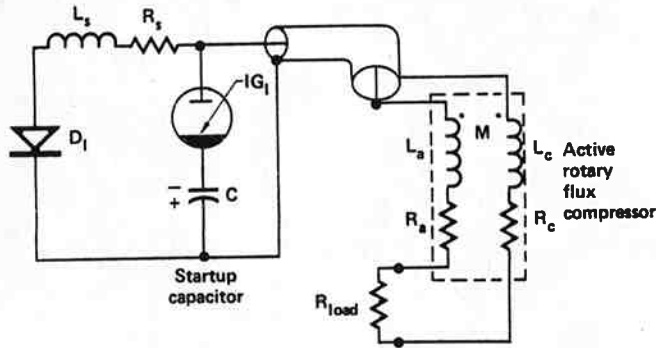


Fig. 5. Simplified Circuit Diagram

The capacitor bank C is charged negatively to 2.0-3.0 kV. At the same time the ARFC is accelerated from rest to several thousand rpm using a dc motor. A photo-interrupt circuit is used to trigger the ignitron IG, at a specified mechanical angle (usually  $\theta_m = -\pi/2$ ) after the trigger circuit has been armed by the operator. The capacitor bank is then discharged through the ARFC. At voltage reversal the diode array D<sub>1</sub> becomes forward biased and crowbars the capacitor bank and ignitron. The current then rises as the armature flux is compressed.

A series of short circuit tests were performed, starting at 2,400 rpm with a startup capacitor of 175  $\mu$ F, 2.0 kV. Results of initial short-circuit tests (up to 3,000 rpm, 1 peak ~ 7,670 A) and flash-lamp load tests have been published previously.<sup>6</sup> In order to verify computer circuit analysis models, and to investigate the effects of magnetic saturation, we decided to perform additional short circuit tests before rewinding the machine. The goal of the second set of tests was to reach a peak current of 16 kA from 3,600 rpm using a 700  $\mu$ F bank at 2.5 kV. A digest of test results is given in Table II.

TABLE II  
Short Circuit Test Results

Circuit Parameter	Units	Run No. 34	Run No. 36
		Minimum Pulse Width	Maximum Pulse Width
Rotor inertia	J-s <sup>2</sup>	0.39	0.39
Rotor speed	rpm	5600	5680
Bank capacitance	$\mu$ F	182	369
Bank voltage	kV	2.5	3.0
Injection current	kA	1.01	1.81
Peak current	kA	17.1	25.6
Pulse width (FWHM)	$\mu$ s	590	791

A photograph of the machine current (Run No. 36) oscillograph trace is shown in Figure 6. Note the low-level second peak.

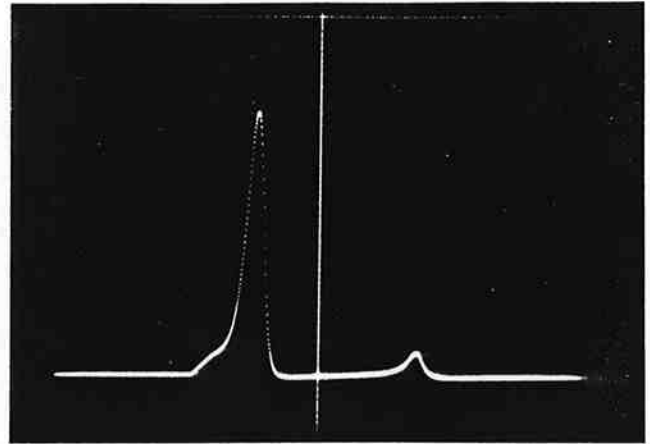


Fig. 6. Machine Current - Run No. 36

## Conclusions

The ARFC was fabricated to verify that a fully laminated rotor and stator assembly would provide the inductance variation required to obtain significant energy gain in larger machines of similar construction. An unsaturated inductance variation of 46.9 was demonstrated. In addition the tests demonstrated (1) current gain in excess of 15:1 at 63 percent of first rotor critical, (2) pulse width (full width, half max) of <600  $\mu$ s at 17 kA, (3) ability of computer codes to match measured waveforms, and (4) saturation effects less severe than worst-case model. It is important to note that the ARFC, although designed as a static measurement device, has generated 25.6 kA at 5,680 rpm with no significant damage to the machine.

Circuit analyses of larger-scale machines (8-10 MJ) indicate that energy gains in excess of 10:1 are technically feasible for resistive loads, such as flash-lamps, for pulsedwidths ranging from 500  $\mu$ s to 750  $\mu$ s.

This work was funded by the Lawrence Livermore National Laboratory and the Texas Atomic Energy Research Foundation.

## References

- W. L. Bird et al., "Detailed Design, Fabrication, and Testing of an Engineering Prototype Compensated Pulsed Alternator," Final Report, Lawrence Livermore Laboratory P.O. No. 3325309, March 1980.
- K. M. Tolk, "The Design and Fabrication of a Second-Generation Compensated Pulsed Alternator," Final Report, Naval Surface Weapons Center Contract No. N60921-78-C-A249, Conceptual Design Phase, Jan. 1980.
- W. L. Bird et al., Final Report, Lawrence Livermore Laboratory P. O. No. 8030909, March 1981.
- W. L. Bird et al., Monthly Report, Lawrence Livermore Laboratory P.O. No. 8030909, July 1980.
- Jayesh A. Parekh, et al., "Space Harmonic Analysis of Magnetic Fields in a Compensated Pulsed Alternator or an Active Rotary Flux Compressor," proc. of this conference.
- W. L. Bird, oral presentation, CEM-UT--LLNL Compensated Pulsed Alternator Seminar, Lakeway Inn, Austin, TX, November 18-19, 1980.